A Density Functional Theory Study of the Charge State of Hydrogen in Metal Hydrides

Shela Aboud and Jennifer Wilcox*

Department of Energy Resources Engineering, Stanford University, Stanford, California 94305

Received: December 14, 2009; Revised Manuscript Received: April 21, 2010

Density functional theory and Bader charge analyses were used to investigate the charge state of hydrogen in vanadium, niobium, tantalum, palladium, and niobium−palladium alloys. Over a range of concentrations and hydrogen-site configurations, it is found that hydrogen consistently acquires a net charge of between approximately $-0.51e$ and $-0.64e$ in the pure group 5 metals compared with a significantly smaller value of $0.3e$ in palladium. Although there is indirect evidence that the electronic charge plays a role in the solubility and diffusivity of hydrogen in the group 5 metals, this is the first work to quantify the value of the charge. Hydrogen tends to migrate to regions of the metal lattice that minimize its overall charge density, which generally corresponds to the T-site in the bcc metals. It is found that the charge of hydrogen at the O-site of vanadium can be slightly lower due to lattice deformation and may explain the occupation of both T- and O-sites in vanadium hydrides.

Introduction

Investigating the physical mechanisms governing hydrogen transport in the group 5 metals is important not only for their application for improving hydrogen purification systems, fuel cells, and hydrogen storage materials but also because they can be used as representative models to understand the electronic properties of light interstitial atoms in metals. Although, the phenomenological behavior of hydrogen in the group 5 transition metals has been extensively studied both theoretically and experimentally for more than 30 years,[1] a fundamental understanding of the role that electronic charge plays in metal hydrides is still incomplete.

Group 5 materials, in general, can dissolve large amounts of interstitial hydrogen with a maximum reached experimentally of two hydrogen atoms per metal atom in vanadium and niobium.[2] At low hydrogen concentrations, the bcc metal hydride is described by a disordered α phase where hydrogen randomly occupies the tetrahedral sites (T-sites) of the host lattice, which generally has a lower electron density compared with the octahedral site (O-site).[3] The group 5 metals all have a lower electronegativity than hydrogen, and electrons will be attracted from the host metal to the hydrogen, forcing it to migrate toward the lower electron density regions. The electronegativity of hydrogen is 2.2, whereas for vanadium, niobium, and tantalum, it is 1.63, 1.6, and 1.5, respectively. In comparison, in fcc metals with higher electronegativities, the hydrogen atom will tend to release its electron more readily and will occupy the O-sites, which have a relatively higher electron density.[3] At increased concentrations of hydrogen, the group 5 hydrides are described by an ordered β phase. At short hydrogen−hydrogen distances, there is also evidence of a repulsive interaction that results in site blocking that decreases the partial configuration entropy compared to a purely random hydrogen distribution[4] and ultimately leads to the formation of the ordered β phases. Below room temperatures, the transition to the β phase occurs at approximately 70% hydrogen for niobium and at 50% hydrogen for vanadium and tantalum, although the ordered β phase can coexist with the α phase at lower hydrogen concentrations. In vanadium, for concentrations above 50% hydrogen, both the T- and the O-sites are found to be occupied with 90% T-sites and 10% O-sites.[5] This mix of site occupation in the vanadium hydride β-phase state has been attributed to both the high electronegativity of vanadium[6] and the geometric effects resulting from a large distortion of the vanadium hydride lattice.[7] In this work, there is evidence that hydrogen is more stable in the O-site of vanadium compared with niobium and tantalum because of a lower charge transfer between the vanadium and the hydrogen atoms at the O-site, which results in a lower hydrogen−hydrogen repulsion energy.

Experimental measurements of the heats of solution of hydrogen in substitutional metal alloys have shown the general trend that solubility is governed mainly by electronic effects in group 5 metals and by volume effects in palladium.[4] Although this data suggests that the electron density plays a more significant role in the absorption behavior of hydrogen in group 5 than in palladium, no quantitative information has been given regarding the actual form of the electronic effects. Describing the solubility of hydrogen in palladium, Wagner[8] derived a nonideal form of Sieverts' law that accounts for the electronic properties of dissolved hydrogen, and later, Brodowsky[9] extended this model to include the long-range elastic strain contribution to the excess chemical potential. The elastic strain field results from the lattice distortion and gives rise to a long-range attractive interaction between the dissolved hydrogen, which is essentially independent of the local composition in the lattice.[10] The volume expansion resulting from the interstitial hydrogen has been measured at a consistent 3 Å^3 per hydrogen atom[4] for a wide range of metals and metal alloys, including those of group 5 and palladium.[11] Recent pressure−composition−temperature (PCT) measurements of hydrogen solubility in pure niobium and in Pd−26 % mol Ag alloy membranes at 773 K concluded that, although hydrogen dissolution in the PdAg alloy[12] follows the ideal behavior of Sieverts' law up to pressures of 1 MPa, hydrogen in niobium did not follow the ideal behavior for pressures greater than 0.003 MPa.[13] Taking into account the electronic and elastic strain effects in the nonideal form of Sieverts' law could explain the deviations from the ideal hydrogen solubility in

* To whom correspondence should be addressed. E-mail: jen.wilcox@stanford.edu.

10.1021/jp911811r © 2010 American Chemical Society
Published on Web 05/26/2010

niobium; however, it is clear that the behavior of hydrogen is different in niobium compared with that in palladium.

Hydrogen diffusion occurs through transitions between adjacent interstitial T- or O-sites depending on the stability of the sites in the metal. Diffusion coefficients in the group 5 metals are larger than any other besides iron and as much as an order of magnitude greater than palladium.[14] In general, diffusivities through bcc metals are believed to be faster than in fcc purely from a geometric standpoint given the shorter distances between adjacent stable binding sites. Experimental work and density functional theory (DFT) calculations of hydrogen in fcc and bcc phases of PdCu alloys have shown that hydrogen in the bcc structures has a diffusivity nearly 2 orders of magnitude greater than in the fcc phase.[15] Given the short distances between the stable T-sites in the group 5 metals (~1.5 Å in vanadium and 1.65 Å in niobium and tantalum), the fast diffusivity has been attributed to hydrogen tunneling phenomena.[11,16] As hydrogen moves between T- or O-sites, the surrounding metal atoms will distort from their equilibrium positions, lowering the hydrogen *self-trapping* energy, which is also what gives rise to the elastic strain field. The energy levels associated with the initial and final interstitial sites are no longer equivalent, and the hydrogen tunneling probability can be significantly reduced because of the loss of energy conservation.[15,17] Thermal fluctuations may compensate for the self-trapping energy, resulting in phonon-assisted tunneling at low temperatures,[15] but at higher temperatures, especially above room temperature, the diffusion of hydrogen is adequately described by classical hopping between stable interstitial sites.

Although the electronic states of metal hydrides have been studied extensively, the actual charge on the hydrogen atom has not been well-characterized. Overall, the current accepted picture of the electronic structure of transition-metal hydrides is that the electrons of the hydrogen atom are delocalized by exchange interactions with the high-density d states at the Fermi level of the metal and become essentially electronically screened protons,[18] but to the authors' knowledge, there is no literature directly quantifying the amount of electronic charge assumed by the hydrogen atom in the group 5 materials. The reason for the lack of theoretical and computational information regarding the hydrogen charge most likely stems from difficulties in partitioning the charge density distribution and assigning it to the respective atoms. Charge-partitioning schemes, such as the Mulliken population analysis, depend on the assignment of the basis set to the atoms, so it is not applicable to plane-wave methods, which are needed for periodic structure simulations. Most of the previous work alluding to charge has been indirect. Using band structure and density of states (DOS) calculations of metal hydrides, Switendick[19] proposed a dual mechanism in which the electronic structure of the metal hydride arises from both an anionic model where the addition of low-lying hydrogen states gain electrons from the host atoms and a protonic model of hydrogen in which the Fermi level of the metal shifts to higher energies to accommodate the addition of the hydrogen electrons. In addition, more recent DFT simulations by Gupta[20] using augmented plane-wave (APW) calculations of zirconium hydride and niobium hydride showed qualitative evidence of electron charge transfer from the metal lattice to the hydrogen atom through DOS calculations. Although the DOS results do not allow for the extraction of the specific charge gained by the hydrogen atom, Gupta's work was able to confirm that the hydrogen is not purely anionic, given that the low-lying hydrogen states overlap the metal d, p, and s states. In this work, the DOS analysis also shows the strong interaction between hydrogen and the metal states.

In this work, the atomic charge of the hydrogen is calculated using a Bader charge analysis.[21] Within the approach proposed by Bader, the continuous electron density is partitioned into regions bounded by the minima of the charge density. Using this method in conjunction with the DFT calculations of the electron density, hydrogen is found to acquire a significant and rather consistent charge in vanadium, niobium, and tantalum over a range of concentrations and binding sites. Comparisons are made with the charge density of interstitial hydrogen in palladium and palladium−niobium alloys to demonstrate the mechanistic difference of hydrogen bonding in the group 5 metals. To the authors' knowledge, this is the first time, experimentally or theoretically, that the charge of hydrogen has been quantitatively measured in vanadium, niobium, and tantalum.

In the following sections, the DFT and Bader charge analyses are described and results are presented for both the low concentration region, where the lattice distortion is minimal, and higher concentrations where the strain field plays a larger role in the hydrogen absorption process in the group 5 metal hydrides. Results are also given for the charge of interstitial hydrogen in pure palladium and in a niobium lattice with different nearest-neighbor concentrations of palladium atoms. A DOS analysis is then carried out to further understand the role of charge density on the hydrogen−metal lattice interactions. Finally, a discussion about the correlation between the stability of hydrogen at various interstitial sites and the corresponding charge density is presented.

Computational Methodology

Density functional theory calculations were performed with the Vienna ab initio Simulation Package (VASP)[22] using the projector augmented wave (PAW) method[23] to describe the ion−electron interactions. Electron exchange-correlation functionals were represented with the generalized gradient approximation (GGA), and comparisons were made with two nonlocal corrections, Perdew and Wang (PW91),[24] and Perdew, Burke, and Ernzerhof (PBE).[25] In general, it is difficult to determine the correct PAW pseudopotential parameters for highly electronegative elements, such as vanadium, niobium, and tantalum. In fact, the 4p orbitals from the core region had to be treated as valence electrons in order to obtain the correct physical bulk properties and electronic structure for niobium,[26] whereas the semicore p states remain fixed for the vanadium and tantalum pseudopotentials. For all calculations, a plane-wave expansion cutoff of 350 eV was used and the surface Brillouin zone integration was calculated using a $7 \times 7 \times 7$ Monkhorst−Pack scheme.[27] A Methfessel and Paxton[28] Gaussian smearing of order 1 was used with a width of 0.2 eV to accelerate the convergence of the total energy calculations.

The bulk vanadium, niobium, and tantalum crystal lattices were modeled with a periodic $2 \times 2 \times 2$ bcc cell corresponding to a supercell of 16 atoms. Simulations were run for a range of hydrogen concentrations corresponding to $c = \mathrm{H/M} = 0.0625$, 0.125, 0.25, and 0.5 (where M = vanadium, niobium, or tantalum). The equilibrium lattice constant was calculated for the bulk crystal and then reoptimized for the metal hydrides with the hydrogen atoms placed at the specific interstitial locations. All atoms in the cell were then allowed to relax to their equilibrium positions. The relaxation was performed with the conjugate-gradient algorithm until the force on all the unconstrained atoms was less than 0.01 eV/Å. The absorption

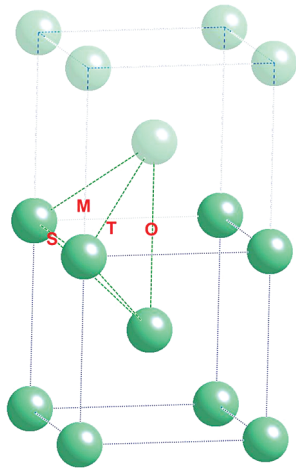

Figure 1. Two unit cells of a bcc lattice showing the T- and O-site locations of interstitial hydrogen. Dashed lines show T-site boundaries.

energy of hydrogen at the various stable positions was calculated with the expression

$$E_{abs} = E_{bulk+H} - E_{bulk} - 0.5E_{H_2} - E_{ZPE} \quad (1)$$

where the energy terms on the right-hand side represent, in order, the metal with hydrogen absorbed at the appropriate site, the bulk metal, and gas-phase hydrogen. For absorption at the T-sites, the correction due to the change in zero-point energy (ZPE) between the free hydrogen gas and the interstitial hydrogen was also included. The ZPE for interstitial hydrogen was determined by fixing the metal atoms and then using the forces generated from displacing the hydrogen atoms to calculate the Hessian matrix. By placing hydrogen at both T- and O-sites, denoted in Figure 1, and calculating the corresponding absorption energy, the stability of interstitial hydrogen can be explicitly determined. The strength of the absorption energy at a given location is a measure of the stability of that site and provides information about the solubility of hydrogen in the given material. Large negative absorption energies signify stable binding, whereas positive energies can be inferred as a site that will tend to be unoccupied. The energy of the gas-phase hydrogen dimer was calculated with a $10 \times 10 \times 10$ cell and benchmarked against experimental bond lengths and vibrational frequencies. The NbPd alloy simulations were carried out by replacing the niobium atoms with palladium atoms at specific nearest-neighbor locations around the T- and O-sites of hydrogen in a 16-atom supercell at $c = 0.0625$. On the basis of the phase diagram of NbPd alloys, the total concentration of the palladium atoms was kept below 25% to ensure that the bcc structure of niobium is not compromised.[29]

The charge distribution from the DFT calculations was partitioned and assigned to the individual atoms using the Bader charge analysis. When using PAW pseudopotentials, a sufficient number of the core electrons must be included to reproduce the correct charge density with a maximum around each atom; otherwise, the Bader charge analysis will not give correct results. To avoid possible errors in the Bader charge from the use of the effective core potentials, either additional s- or p-core states can be treated as valence states, which is done for niobium, or the electron density from both the valence and the core electrons can be used in the calculation of the Bader volumes as was done for the vanadium and tantalum hydrides in this work. Calculations of the Bader charge without using the core electrons for vanadium and tantalum overestimated the hydrogen charge by approximately 50−200%. The accuracy of the Bader charge has been validated by running simulations with a finer mesh, and a reduction in the mesh size by a factor of 2 in each of the three dimensions results in a change of the Bader charge of only ∼1%.

TABLE 1: Group 5 Lattice Constant and Gas-Phase Hydrogen Parameters

	PW91	PBE	exp.[30]
V lattice constant (Å)	2.98	2.98	3.03
Nb lattice constant (Å)	3.32	3.32	3.30
Ta lattice constant (Å)	3.32	3.32	3.30
H_2 bond length (Å)	0.75	0.75	0.74
H_2 vib. frequency (cm^{-1})	4321.71	4329.77	4401.21

TABLE 2: Hydrogen Absorption Energy and Volume Expansion in Vanadium, Niobium, and Tantalum for Different Local Exchange Models

		T-site		O-site	
system		E_{abs} (eV)	v_H (Å^3/H)	E_{abs} (eV)	v_H (Å^3/H)
$V_{16}H$	PW91	−0.217	2.991	−0.007	3.006
	PBE	−0.280	3.303	−0.075	2.957
$Nb_{16}H$	PW91	−0.293	2.895	0.039	2.841
	PBE	−0.350	3.358	−0.022	2.793
$Ta_{16}H$	PW91	−0.279	2.503	0.087	3.230
	PBE	−0.341	3.221	0.014	3.129

Results and Discussion

Gas-Phase Hydrogen and Bulk Metal Properties. The equilibrium lattice constants for the group 5 materials and bond length and vibrational frequency of gas-phase hydrogen are calculated to calibrate the DFT parameters and show excellent agreement with measured experimental data, as shown in Table 1. Niobium and tantalum have identical lattice constants measured experimentally, which is also found for the DFT calculations and agrees to within 0.6% for both PW91 and PBE nonlocal corrections. Vanadium has a smaller lattice differing from experiment by approximately 1%. As defined by eq 1, to determine the absorption energy of hydrogen at an interstitial site of the host metal, the energetic contribution from the stable state of hydrogen must be subtracted from the total energy of the metal hydride. The stable state of hydrogen corresponds to the gas-phase H_2, and Table 1 shows that the corresponding simulated bond length and vibrational frequency compared with experiment and both are within 2%.[30]

Absorption Energy of Interstitial Hydrogen. Hydrogen atoms are placed at different interstitial locations in the bcc lattice of the group 5 materials under a range of concentrations, and the equilibrium lattice constant is reoptimized. The local positions of the hydrogen and metal atoms are then allowed to relax. At low hydrogen concentrations of $c = 0.0625$, the lattice constant does not change from the pure material, and as shown in Table 2, the absorption energies of hydrogen at the T-site in the group 5 metals are found to be the most stable and overall compare well to the experimentally measured heats of solution of −0.28, −0.35, and −0.39 eV for vanadium, niobium, and tantalum,[4] respectively, with the best agreement coming from the simulations with the PBE model used as the local potential. The vanadium and niobium are in much better agreement with experiment than the tantalum, which has an absorption energy approximately 12% lower than the heat of solution at the lowest hydrogen concentration. Also shown in Table 2 is the DFT-calculated volume expansion due to hydrogen (v_H) and compares well with the experimentally determined values of 2.64, 3.13,

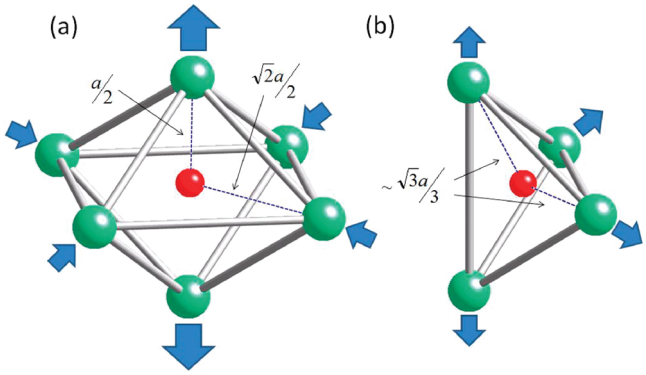

Figure 2. Schematic of the lattice distortion caused by the hydrogen atom at the (a) O-site and (b) T-site in the group 5 metal hydrides. The size and orientation of the arrows correspond approximately to the amount and direction of the strain.

and 2.80 Å^3/H atom, for hydrogen at the T-sites of vanadium, niobium, and tantalum, respectively.[31] The simulated volume expansion is calculated by measuring the change in volume of the 16-atom unit cell with the inclusion of hydrogen at the T-site. In general, the PBE nonlocal correction gives the best agreement to experiment and follows the trend between the different metals for the T-site occupation and is exclusively used in subsequent results unless otherwise specified.

The total amount of expansion of the lattice is similar when hydrogen is located at the T- or O-site, but the way in which the surrounding lattice deforms to accommodate the hydrogen is very different. The O-site absorption behavior is particularly interesting to examine for the vanadium system because of the presence of both T- and O-site occupation at high concentrations ($c \geq 0.5$). In a bcc structure, the four nearest metal atoms are almost the same distance from the T-site, while the distances from the position of the O-site to the six nearest metal atom neighbors is less symmetric. As shown in Figure 2a, the four neighbors in the plane of the O-site are at a distance of $(a\sqrt{2})/2$, while the two metal atoms out of the plane are closer at a distance of $a/2$, where a is the lattice constant of the metal. In comparison, as shown in Figure 2b, the four nearest neighbors surrounding the T-site are all at a distance of approximately $(a\sqrt{3})/3$. When hydrogen is placed at the T-site, all the neighboring atoms expand away from the hydrogen uniformly. The hydrogen-induced displacement is much different at an O-site occupancy, and the two out-of-plane metal atoms expand away from the binding site, while the other four metal atoms contract toward hydrogen by approximately 83, 71, and 76% in vanadium, niobium, and tantalum, respectively. In the group 5 metals, hydrogen acts in such a way as to make the O-site more symmetric, and in the case of vanadium, which has the largest lattice distortion, hydrogen may be helping to stabilize the binding site. In comparison, in metals, such as palladium, with an fcc structure, the O-site is more symmetric than the T-site.

To examine the effects of increased hydrogen concentration, two, four, and eight hydrogen atoms are placed in 16 metal-atom unit cells at T-site locations in such a way as to maximize the distance between the neighboring hydrogen atoms. A comprehensive study of all of the possible ordered and disordered configurations of the hydrogen T-site occupation (and O-site occupation in the case of vanadium) is beyond the scope of this work, and only a finite number of structures are examined in order to understand and identify trends in the hydrogen absorption process. For niobium and tantalum, an additional hydrogen configuration at $c = 0.5$ is simulated, which is based on the tantalum hydride neutron diffraction measurements of Somenkov et al.[5] At increased values of hydrogen content, the metal hydride lattice constant changes compared to the lattice constant of the pure metal, as shown in Table 3. At the maximum concentration investigated in this work ($c = 0.5$), the lattice constant changes by approximately 2% in the case of niobium and tantalum and approximately 3% for vanadium. The absorption energies of hydrogen are calculated using eq 1, and the results of the Bader charge analysis (described in the following section) are also shown in Table 3. Below hydrogen concentrations of $c = 0.25$ in all three group 5 metals, the absorption energy of the individual hydrogen atoms increases as the concentration increases. This is consistent with a long-range attractive interaction between the hydrogen atoms at low concentrations. As the hydrogen content increases, the lattice expands, enhancing the absorption of subsequent hydrogen due to the lattice strain field.

At higher concentrations, the picture changes and increasing the hydrogen concentration in vanadium and tantalum does not result in an increased interaction between the hydrogen and the metal lattice. As shown in Table 3, the binding energy weakens for $c = 0.5$ for these two materials. This is consistent with the existence of a competing short-range repulsive interaction between neighboring hydrogen atoms, which ultimately is responsible for the creation of the β phase in these two materials at $c = 0.5$. In comparison, the absorption energy of hydrogen in the niobium hydride, which does not undergo a transition to the β phase until the hydrogen concentration reaches $c = 0.7$, does not show a reduction in the hydrogen−metal atom interaction at $c = 0.5$.

Also shown in Table 3 is the absorption energy of hydrogen in niobium and tantalum for two different spatial configurations of the hydrogen atoms at $c = 0.5$, which corresponds to a uniform distribution consistent to results of neutron diffraction experiments of tantalum hydride by Somenkov et al.[5] As can be seen in Table 3 for tantalum at $c = 0.5$, the absorption energy of hydrogen is dependent on the position of neighboring

TABLE 3: Bader Charge and Hydrogen Absorption Energy for Different Concentrations at the T- and O-Site of Vanadium, Niobium, and Tantalum

	V			Nb			Ta		
c = H/M[a]	a (Å)	Q_H (e)	E_{abs} (eV)	a (Å)	Q_H (e)	E_{abs} (eV)	a (Å)	Q_H (e)	E_{abs} (eV)
0.0625 (O)	2.98	−0.509	−0.076	3.32	−0.612	−0.022	3.32	−0.622	0.014
0.0625 (T)	2.98	−0.590	−0.281	3.32	−0.601	−0.350	3.32	−0.603	−0.341
0.125 (T)	3.01	−0.606	−0.330	3.35	−0.617	−0.367	3.33	−0.614	−0.379
0.25 (T)	3.03	−0.598	−0.386	3.37	−0.626	−0.426	3.35	−0.608	−0.427
0.5 (T)	3.08	−0.633	−0.280	3.41	−0.635	−0.449	3.39	−0.617	−0.390
0.5[b] (T)				3.41	−0.632	−0.397	3.39	−0.603	−0.417

[a] M = V, Nb, or Ta. [b] Hydrogen configuration based on the work of Somenkov et al.[5]

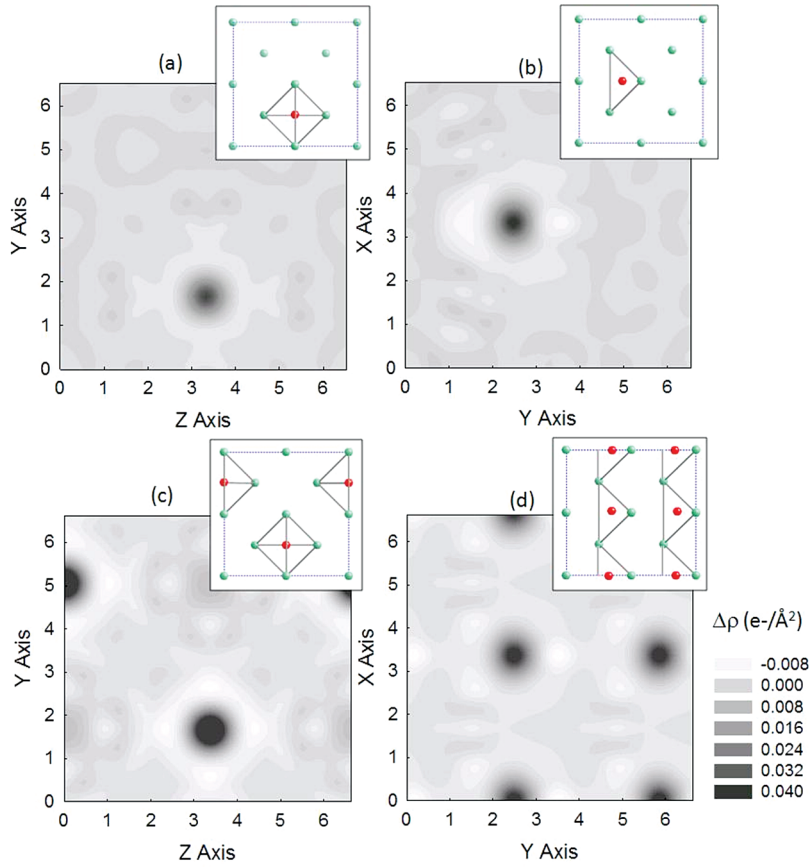

Figure 3. Spatial distribution of the change in electron density in niobium for a hydrogen concentration of (a, b) $c = 0.0625$ and (c, d) $c = 0.25$ along the Y and Z directions, respectively.

hydrogen atoms and the configuration corresponding to the experimental work is the more stable one. Although it is important to note that not all possible configurations were simulated and it is possible that there are other structures that could result in a stronger interaction for any of the metal hydride systems, the balance between the long-range attractive interaction due to the deformation of the lattice and the short-range repulsive interaction between neighboring hydrogen atoms does appear to influence the calculated absorption energies, at least for vanadium and tantalum.

Hydrogen Charge Density. The Bader charge of hydrogen at the T-site of all three metals is also shown in Table 3 and is found to be between approximately $-0.51e$ and $-0.64e$ for all hydrogen concentrations considered. This is consistent with the relative similarities of the electronegativities of the three materials at values of 1.63, 1.6 and 1.5 for vanadium, niobium, and tantalum, respectively. In comparison, using the same computational methodology, the charge of a hydrogen atom at the O-site of palladium is calculated to be $0.03e$ at a concentration of $c = 0.037$. Although consistent, there are small variations in the calculated values of the Bader charge of hydrogen in the group 5 materials over the range of simulated concentrations. In the case of niobium, the charge increases with increasing hydrogen concentration. The charge of hydrogen in vanadium and tantalum, on the other hand, increases from hydrogen concentrations of $c = 0.0625$ to $c = 0.125$ and then decreases at $c = 0.25$. This reduction in the hydrogen charge could be an indication of the onset of the short-range hydrogen−hydrogen interaction. Also, in tantalum at concentrations of $c = 0.50$, the hydrogen charge (along with the absorption energy, as discussed above) is dependent on the local configuration of the hydrogen atoms, and the configuration that minimizes the charge density corresponds to the one that is the most stable because of a reduction in the repulsive electrostatic interaction between the neighboring hydrogen atoms. This trend is also observed when the hydrogen atom is located at the O-site of the niobium or tantalum lattice. The Bader charge of hydrogen at the O-site of niobium and tantalum compared with the T-site is higher by approximately 2% and 3%, respectively. Interestingly, the Bader charge of hydrogen at the O-site in vanadium decreases by 5% at a concentration of $c = 0.0625$ compared with that at the T-site. Because the hydrogen charge does not increase at the O-sites in vanadium compared to the T-sites, this could be a factor in why both interstitial sites are found to be occupied at high hydrogen concentrations.

To investigate the spatial distribution of the charge density resulting from interstitial hydrogen, the charge density difference averaged along the z axis is calculated with the expression

$$\Delta\rho(x, y) = \frac{1}{L_Z}\int \mathrm{d}z[\rho(x, y) - \rho_{\mathrm{bulk}}(x, y) - \rho_{\mathrm{H}}(x, y)] \tag{2}$$

where L_z is the length of the unit cell in the z direction, $\rho(x,y)$ is the average charge density in the (x,y) plane of the niobium lattice with the absorbed hydrogen, $\rho_{\mathrm{bulk}}(x,y)$ is the average charge density in the (x,y) plane with the hydrogen removed, and $\rho_{\mathrm{H}}(x,y)$ is the average charge density with the niobium atoms removed. A similar expression can be written for the average charge density along the x or y axis. A plot of the charge density difference averaged along the different crystallographic axes is shown for hydrogen at the T-site in a niobium lattice in Figure 3a,b at a concentration of $c = 0.0625$ and in Figure 3c,d at a concentration of $c = 0.25$. A positive increase in the charge

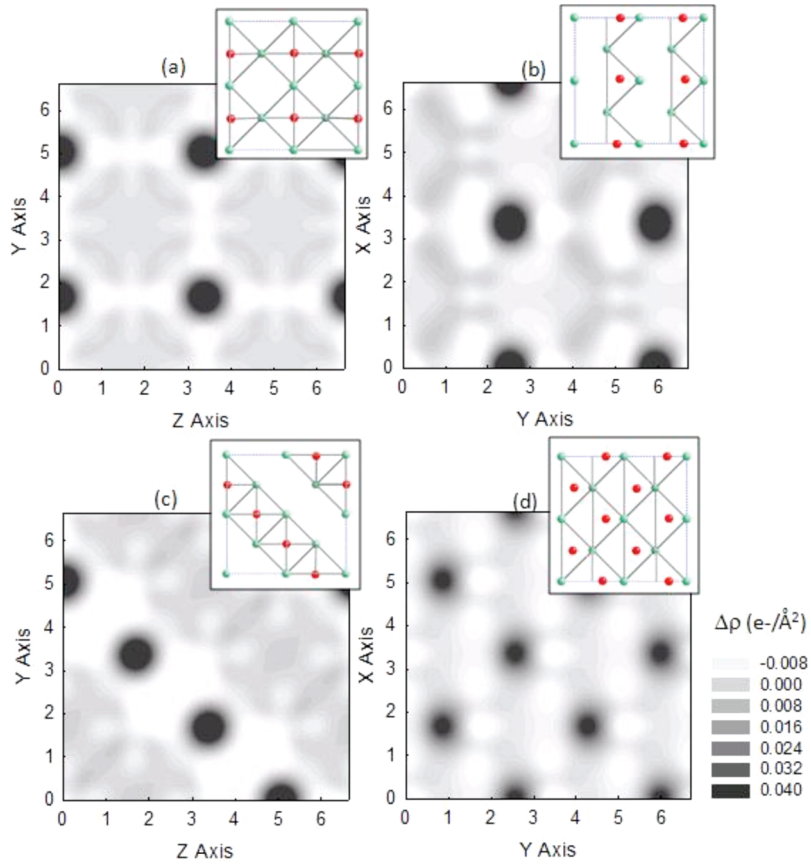

Figure 4. Spatial distribution of the change in electron density in tantalum for a hydrogen concentration of $c = 0.5$ for (a, b) random hydrogen ordering and (c, d) ordering based on neutron-scattering experimental work of Somenkov et al., along the Y and Z directions, respectively.

density represents an increase in the number of electrons, and the negative regions in the plots occur due to the accumulation of electrons surrounding the hydrogen atom. The localization of the charge and the increased charge at $c = 0.25$ are clearly seen in the figures. The charge density difference for the two different hydrogen configurations in tantalum is shown in Figure 4. A uniform distribution that maximizes the distances between the neighboring hydrogen atoms is shown in Figure 4a,b, and a hydrogen ordering that reflects neutron-scattering measurements by Somenkov et al.[5] is shown in Figure 4c,d. Although the neighboring hydrogen atoms are actually closer together in the experimental configuration, the charge they acquire from the interactions with the metal lattice is smaller, which reduces the short-range repulsive interaction, making hydrogen more stable than for the uniform configuration.

Effects of Alloying. As a comparison, DFT calculations and a Bader charge analysis were also carried out for interstitial hydrogen in NbPd alloys to compare the trends in the hydrogen charge versus concentration. To understand the influence of the local concentration of palladium atoms on the stability and size of the individual hydrogen-binding sites, the hydrogen is placed at a T- or O-site in the 16-atom niobium supercell and different nearest-neighbor atoms are replaced with palladium. The stabilities of the alloy compositions examined in this work are determined using the expression for the formation energy

$$\Delta E_f = E(Nb_xPd_{1-x}) - xE(Nb) - (1 - x)E(Pd) \quad (3)$$

where the first term is the energy of the alloy and the second and third terms are the contributions to the energy from pure Pd and Nb systems, respectively. The stability of the alloys increases with increasing Pd concentration from approximately

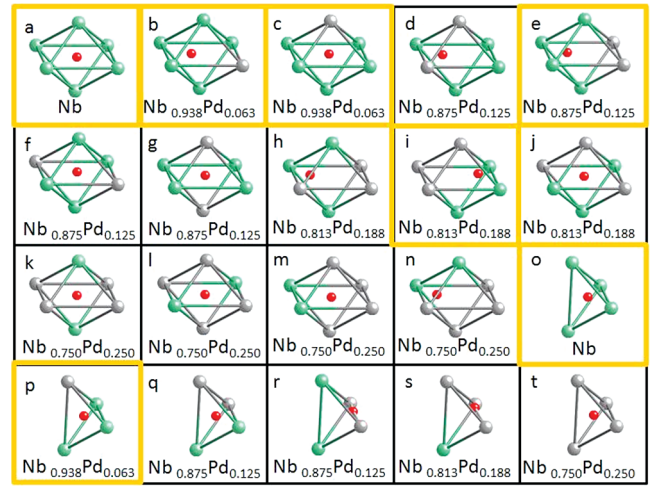

Figure 5. Final configuration of interstitial hydrogen in the varying local compositions of neighboring atoms in NbPd alloys. Highlighted boxes signify the stable configurations.

−2.34 eV at $x = 0.938$, −4.35 eV at $x = 0.875$, −5.89 eV at $x = 0.813$, and to −7.50 eV at $x = 0.750$. Shown in Figure 5 is a plot of all the final hydrogen configurations in the NbPd alloys. As can be seen from the position of the hydrogen atom, depending on the local concentration of palladium, the final binding site is not always the same as the initial one. The diagrams highlighted in yellow denote the structures that are energetically stable, and the corresponding binding energy for these configurations is shown in Table 4. In all cases, the strongest binding energy corresponds to the T-site of the pure niobium, and the palladium dopant atoms in the nearest-neighbor shell act to weaken the interaction. Also shown in Table 4 is

TABLE 4: Absorption Energy and Bader Charge of Interstitial Hydrogen in NbPd Alloys

alloy composition	configuration from Figure 5	Q_H (e)	E_{abs} (eV)
$Nb_{0.938}Pd_{0.063}$ (O-site)	b	−0.5206	−0.122
$Nb_{0.938}Pd_{0.063}$ (O-site)	c	−0.4218	−0.008
$Nb_{0.875}Pd_{0.125}$ (O-site)	d	−0.3996	0.015
$Nb_{0.875}Pd_{0.125}$ (O-site)	e	−0.5468	−0.162
$Nb_{0.875}Pd_{0.125}$ (O-site)	f	−0.5112	0.439
$Nb_{0.875}Pd_{0.125}$ (O-site)	g	−0.2845	0.148
$Nb_{0.813}Pd_{0.188}$ (O-site)	h	−0.4911	0.208
$Nb_{0.813}Pd_{0.188}$ (O-site)	i	−0.4328	−0.031
$Nb_{0.813}Pd_{0.188}$ (O-site)	j	−0.3354	0.264
$Nb_{0.750}Pd_{0.250}$ (O-site)	k	−0.5021	0.132
$Nb_{0.750}Pd_{0.250}$ (O-site)	l	−0.2454	0.718
$Nb_{0.750}Pd_{0.250}$ (O-site)	m	−0.2314	0.152
$Nb_{0.750}Pd_{0.250}$ (O-site)	n	−0.3597	0.122
$Nb_{0.938}Pd_{0.063}$ (T-site)	p	−0.516	−0.777
$Nb_{0.875}Pd_{0.125}$ (T-site)	q	−0.372	0.148
$Nb_{0.875}Pd_{0.125}$ (T-site)	r	−0.331	0.156
$Nb_{0.813}Pd_{0.188}$ (T-site)	s	−0.226	0.154
$Nb_{0.750}Pd_{0.250}$ (T-site)	t	−0.144	0.231

the charge acquired by hydrogen in each of the final interstitial configurations in the NbPd alloys. As can be seen, the strength of the binding is related to the hydrogen charge where the stability of the site is reduced when hydrogen gains less charge. In the pure niobium lattice, hydrogen gains charge from each of the nearest-neighbor atoms, whereas when the neighboring atoms are replaced with palladium, which has a similar electronegativity as hydrogen, less charge is shared between the lattice and hydrogen, thereby decreasing the binding energy. This demonstrates a fundamental difference between the hydrogen binding mechanism in palladium and niobium (and certainly the group 5 materials in general).

Density of States. The partial DOS is calculated by projecting the electron wave functions onto spherical harmonics centered on the hydrogen and the metal atoms. Although the integral of the DOS up to the Fermi level is proportional to the number of electrons, it is difficult to extract the charge of hydrogen using the partial DOS because the Wigner−Seitz radius used for hydrogen (0.37 Å) is not large enough to ensure that all the charge is included. Plots of the DOS for vanadium, niobium, and tantalum are shown in Figures 6, 7, and 8, respectively, for hydrogen concentrations of $c = 0.0625$ and $c = 0.25$ where the

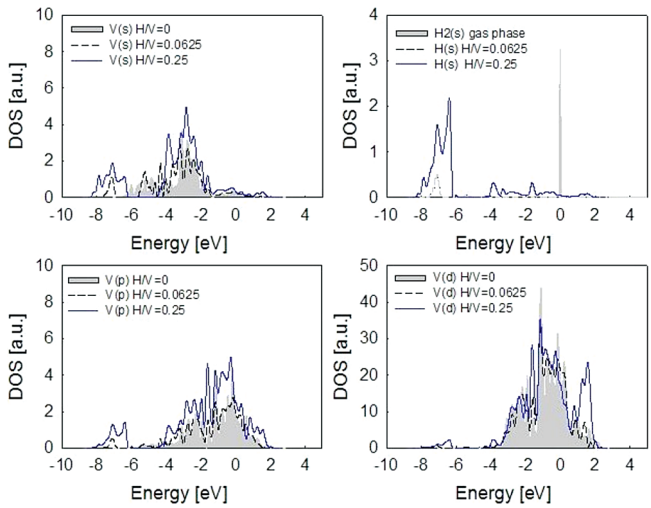

Figure 6. Partial DOS of bulk vanadium compared with hydrogen in vanadium at concentrations of $c = 0.0625$ and 0.25. The Fermi level is located at 0 eV.

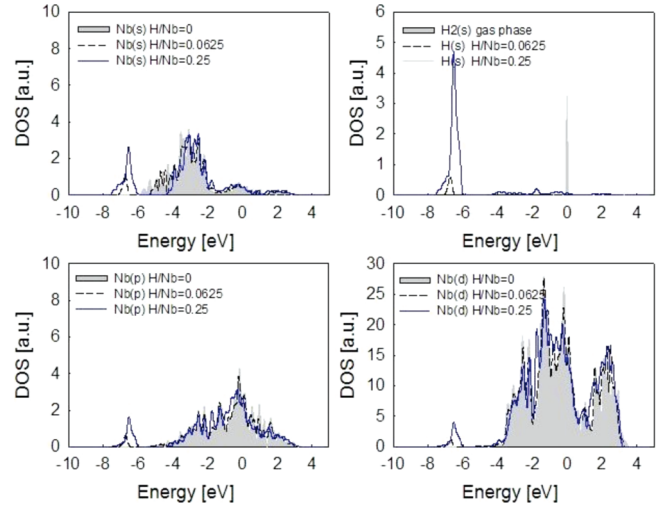

Figure 7. Partial DOS of bulk niobium compared with hydrogen in niobium at concentrations of $c = 0.0625$ and 0.25. The Fermi level is located at 0 eV.

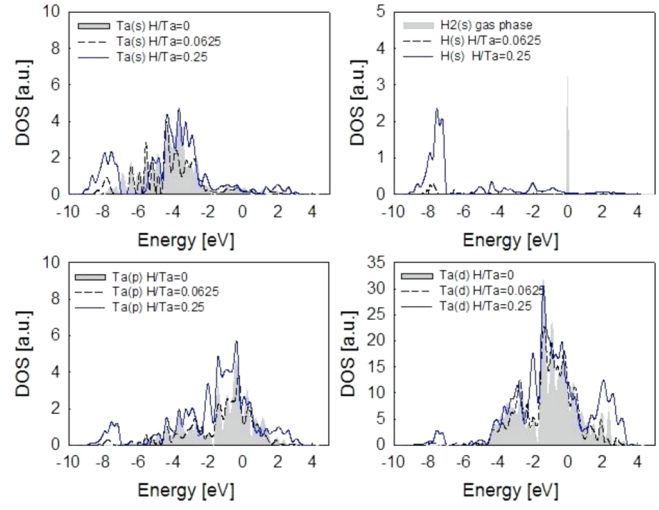

Figure 8. Partial DOS of bulk tantalum compared with hydrogen in tantalum at concentrations of $c = 0.0625$ and 0.25. The Fermi level is located at 0 eV.

Fermi level is located at 0 eV. Also included in the figures is a solid gray region, which represents the partial DOS of the bulk material without the interstitial hydrogen. At low concentrations, the DOS of the s, p, and d states of the metal hydride and the bulk metal are similar except for the addition of the peaks at approximately −7 eV. This is consistent with the results of M. Gupta,[19] which support the existence of an interaction between the hydrogen s and the metal s, p, and d states. At a concentration of $c = 0.25$, a much stronger interaction with the metal atoms can be seen from the additional structure or small peaks between −6 and 0 eV in the hydrogen s state and overlapping metal s, p, and d states. In addition, the hydrogen peak at approximately −7 eV broadens, showing the increased hydrogen−hydrogen interaction. The peaks are most broad in the vanadium hydride, which has both the shortest distance between the interstitial hydrogen and the largest lattice distortion. The hydrogen−hydrogen interaction is weakest in the niobium hydride, as can be seen by the relatively narrow hydrogen peak in Figure 7, compared to the hydrogen peaks in vanadium and tantalum in Figures 6 and 8, respectively. This reduction in the hydrogen−hydrogen interaction further supports the observation of an increased hydrogen repulsive interaction in vanadium and tantalum compared with niobium.

Conclusion

In this study, using DFT and Bader charge analyses, the charge of interstitial hydrogen in vanadium, niobium, and tantalum is found to be between approximately $-0.51e$ and $-0.64e$ over a range of hydrogen concentrations and interstitial hydrogen configurations. The relatively uniform hydrogen charge for the group 5 metals is consistent given the similarities in the electronegativites. In comparison, hydrogen at the O-site of palladium, which has a higher electronegativity, comparable to hydrogen, is found to have a charge of only $0.03e$ at a concentration of $c = 0.037$. This reveals a fundamental difference in the interaction of interstitial hydrogen in the group 5 metals compared with palladium, which is further exemplified by the calculations of the absorption energy and charge of hydrogen in NbPd alloys. In these alloys, the charge gained by hydrogen is reduced as the neighboring niobium atoms in the bcc structure are replaced by palladium atoms, resulting in a less stable interaction. Additional work is ultimately required to define the absolute trends in the correlation between the hydrogen concentration and the absorption energy, but small variations in the charge density do appear to correlate with the stability of hydrogen at the various interstitial sites. At low hydrogen concentrations, the adsorption energy of hydrogen is governed by the long-range attractive interaction through the lattice deformation, and as the concentration increases, the stability of the hydrogen in the adsorption site also increases, as does the charge on hydrogen. As the concentration continues to increase, a short-range repulsive interaction weakens the absorption of hydrogen in vanadium and tantalum. The destabilization of hydrogen seems to correlate to the charge of hydrogen, suggesting that the interaction is, at least partially, electrostatic. In tantalum, the hydrogen configuration that minimizes the Bader charge of hydrogen corresponds to the strongest hydrogen−metal interaction.

References and Notes

(1) See, for instance, the series of books: (a) Alefeld, G., Völkl, J., Eds. *Hydrogen in Metals I*; Topics in Applied Physics; Springer: Berlin, 1978; Vol. 28. (b) Alefeld, G., Völkl, J., Eds. *Hydrogen in Metals II*; Topics in Applied Physics; Springer: Berlin, 1978; Vol. 29.

(2) Schober, T.; Wenzl, H. In *Hydrogen in Metals II*; Topics in Applied Physics; Alefeld, G., Völkl, J., Eds.; Springer: Berlin, 1978; Vol. 29, pp 11−72.

(3) Hauck, J.; Schenk, H. J. *J. Less-Common Met.* **1977**, *51*, 251.

(4) Fukai, Y. *The Metal-Hydrogen System*; Springer: Berlin, 2005.

(5) Somenkov, V. A.; Entin, I. R.; Chervyakov, A. Y.; Shilstein, S.; Chertkov, A. A. *Sov. Phys. Solid State* **1972**, *13*, 2178.

(6) Ross, D. K. In *Hydrogen in Metals III*; Topics in Applied Physics; Wipf, H., Ed.; Springer: Berlin, 1997; Vol. 73, pp 153−214.

(7) Sugimoto, H. *J. Phys. Soc. Jpn.* **1984**, *53*, 2554.

(8) Wagner, C. *Z. Physik. Chem., Abt. A* **1944**, *193*, 386.

(9) Brodowsky, H. *Z. Physik. Chem., Abt. A* **1965**, *44*, 129.

(10) (a) Alefeld, G. *Phys. Status Solidi* **1969**, *32*, 67. (b) Alefeld, G.; Bunsenges, B. *Phys. Chem.* **1972**, *76*, 335. (c) Alefeld, G.; Bunsenges, B. *Phys. Chem.* **1972**, *76*, 746.

(11) Baranowski, B.; Majchrzak, S.; Flanagan, T. B. *J. Phys. F: Met. Phys.* **1972**, *1*, 258.

(12) (a) Sonwane, S.; Wilcox, J.; Ma, Y. H. *J. Chem. Phys.* **2006**, *125*, 184714. (b) Sonwane, S.; Wilcox, J.; Ma, Y. H. *J. Phys. Chem. B* **2006**, *110*, 24549.

(13) Zhang, G. X.; Yukawa, H.; Watanabe, N.; Saito, Y.; Fukaya, H.; Morinaga, M.; Nambu, T.; Matsumoto, Y. *Int. J. Hydrogen Energy* **2008**, *33*, 4419.

(14) Wipf, H. In *Hydrogen in Metals III*; Topics in Applied Physics; Wipf, H., Ed.; Springer: Berlin, 1997; Vol. 73, pp 51−92.

(15) (a) Piper, J. *J. Appl. Phys.* **1966**, *37*, 715. (b) Kamakoti, P.; Sholl, D. S. *J. Membr. Sci.* **2003**, *225*, 145.

(16) Sundell, P. G.; Wahnstrom, G. *Phys. Rev. B* **2004**, *70*, 224301.

(17) Flynn, C. P.; Stoneham, A. M. *Phys. Rev. B* **1970**, *1*, 3966.

(18) Wicke, E.; Brodowsky, H. In *Hydrogen in Metals II*; Topics in Applied Physics; Alefeld, G., Völkl, J., Eds.; Springer: Berlin, 1978; Vol. 29, pp 73−156.

(19) Switendic, A. C. In *Hydrogen in Metals I*; Topics in Applied Physics; Alefeld, G., Völkl, J., Eds.; Springer: Berlin, 1978; Vol. 28, pp 101−130.

(20) Gupta, M. *Phys. Rev. B* **1982**, *25*, 1027.

(21) (a) Henkelman, G.; Arnaldsson, A.; Jónsson, H. *Comput. Mater. Sci.* **2006**, *36*, 254. (b) Sanville, E.; Kenny, S. D.; Smith, R.; Henkelman, G. *J. Comput. Chem.* **2007**, *28*, 899. (c) Tang, W.; Sanville, E.; Henkelman, G. *J. Phys.: Condens. Matter* **2009**, *21*, 084204.

(22) (a) Kresse, G.; Hafner, J. *Phys. Rev. B* **1993**, *48*, 13115. (b) Kresse, G.; Furthmuller, J. *Comput. Mater. Sci.* **1996**, *6*, 15.

(23) (a) Blöchl, P. E. *Phys. Rev. B* **1994**, *50*, 17953. (b) Kresse, G.; Joubert, D. *Phys. Rev. B* **1999**, *59*, 1758.

(24) Perdew, J. P.; Wang, Y. *Phys. Rev. B* **1992**, *45*, 13244.

(25) Perdew, J. P.; Burke, K.; Ernzerhof, M. *Phys. Rev. Lett.* **1996**, *77*, 3865.

(26) VASP support, personal communication.

(27) Monkhorst, H. J.; Pack, J. D. *Phys. Rev. B* **1976**, *13*, 5188.

(28) Methfessel, M.; Paxton, A. T. *Phys. Rev. B* **1989**, *40*, 3616.

(29) Chandrasekhariah, M. S. *Bull. Alloy Phase Diagrams* **1988**, *9*, 449.

(30) Huber, K. P.; Herzberg, G. *Molecular Spectra and Molecular Structure. IV. Constants of Diatomic Molecules*; Van Nostrand Reinhold Co.: New York, 1979.

(31) Peisl, H. In *Hydrogen in Metals I*; Topics in Applied Physics; Alefeld, G., Völkl, J., Eds.; Springer: Berlin, 1978; Vol. 29, pp 53−74.

JP911811R